In-situ tensile testing of propellants in SEM

Influence of temperature

Di Benedetto, Giuseppe L.; van Ramshorst, Marthinus C.J.; Duvalois, Willem; Hooijmeijer, Peter A.; van der Heijden, Antoine E.D.M.

DOI
10.1002/prep.201700178

Publication date
2017

Document Version
Final published version

Published in
Propellants, Explosives, Pyrotechnics

Full Paper

Propellants, Explosives, Pyrotechnics

DOI: 10.1002/prep.201700178

In-Situ Tensile Testing of Propellants in SEM: Influence of Temperature

Giuseppe L. Di Benedetto,[a, b] Marthinus C. J. van Ramshorst,[a, c] Willem Duvalois,[a] Peter A. Hooijmeijer,[a] and Antoine E. D. M. van der Heijden*[a, d]

Abstract: A tensile module system placed within a Scanning Electron Microscope (SEM) was utilized to conduct in-situ tensile testing of propellant samples. The tensile module system allows for real-time in-situ SEM analysis of the samples to determine the failure mechanism of the propellant material under tensile force. The focus of this study was to vary the experimental parameters of the tensile module system and analyze how they affect the failure mechanism of the samples. The experimental parameters varied included strain rate and sample temperature (−54, +25 and +40 °C). Stress-strain diagrams were recorded during the in-situ tensile tests, and these results were coupled with the in-situ images and videos of the samples captured with SEM analysis. The experiments conducted at −54 °C showed a different failure behavior of the propellant sample due to its rigidity at this low temperature, while experiments conducted at +25 and +40 °C displayed a similar failure mechanism. For future testing using this tensile tester, special attention should be given to improved temperature control of the specimen, especially at low temperatures.

Keywords: Propellant · Micromechanical deformation · In-situ tensile testing · In-situ SEM · Temperature effect

1 Introduction

The mechanical response of propellants generally changes as a result of ageing and this can have significant consequences for the safety of the rocket or missile in which the propellant is used. During ignition and operation of a propellant in a rocket motor, pressure is built up in the combustion chamber and in the bore of the propellant grain, resulting in a dynamic mechanical loading of the propellant grain. This mechanical loading may lead to crack initiation and propagation in the propellant grain. This is generally considered as a risk, since the increased burning surface due to the formation of cracks can lead to a cascade effect: the additional surface area which becomes available for burning, will increase the rate at which gaseous products are released. This in turn leads to a higher pressure, which will increase the burning rate. Therefore, it is important to understand the failure mechanism of propellants under varying conditions, so measures can be identified and implemented that prevent the propellant from cracking.

To study the mechanical properties of propellants, macro-level tensile testing has been used extensively, see [1] and literature referred herein. Studying the failure mechanism is usually limited to post-mortem analysis of the ruptured samples. Ramshorst et al. [1] used an in-situ uniaxial tensile test set-up coupled to Scanning Electron Microscopy (SEM) observation. In their study, the mechanical response of a propellant consisting of hydroxyl-terminated polybutadiene (HTPB) filled with ammonium perchlorate (AP) and aluminum (Al) was investigated at three different strain rates, namely 30, 150 and 750 μm/min. The current study extends this work by investigating the effect of temperature on the mechanical behavior and failure mechanism of the same propellant formulation. In-situ uniaxial tensile experiments on propellant samples within a SEM have been performed at a constant strain rate at three different temperatures, i.e. −54, +25 and +40 °C. By combining stress-strain diagrams and in-situ SEM images and videos of the specimens when subjected to tensile loading, the mechanical performance and failure behavior of the solid propellant under uniaxial tensile forces at different temperatures could be investigated.

[a] *G. L. Di Benedetto, M. C. J. van Ramshorst, W. Duvalois, P. A. Hooijmeijer, A. E. D. M. van der Heijden*
Department of Energetic Materials, TNO Defence, Security and Safety, P.O. Box 45, 2280 AA Rijswijk, The Netherlands
**e-mail: antoine.vanderheijden@tno.nl*
[b] *G. L. Di Benedetto*
Advanced Materials Technology Branch U.S. Army RDECOM-ARDEC, Picatinny Arsenal, NJ 07806-5000 USA
[c] *M. C. J. van Ramshorst*
Department of Materials Science and Engineering, Delft University of Technology, Mekelweg 2, 2628 CD Delft, The Netherlands
[d] *A. E. D. M. van der Heijden*
Section Intensified Reaction and Separation Systems
Delft University of Technology
Leeghwaterstraat 39, 2526 CB Delft, The Netherlands
**e-mail: a.e.d.m.vanderheijden@tudelft.nl*

2 Experimental

2.1 Materials

The propellant composition (85 % solid load) was the same as was used in our previous study [1], see Table 1. The aluminum content was 18 wt % of the total composition.

Table 1. Chemical composition of samples used in the experiments.

Binder components (15 wt %)	Solid components (85 wt %)
HTPB R-45HT (binder)	AP 200 μm (70 %)
IDP (inosine diphosphate, plasticizer)	AP 15 μm (30 %)
IPDI (isophorone diisocyanate, curing agent)	Al AS061
Tepanol (bonding agent)	
Flexzone 6H (anti-oxidant)	

The test specimens followed the standard JANNAF C specimen (also known as 'dogbone', see Figure 1), though scaled down by a factor of four, which was necessary because of the size limitations of the tensile test module. It is important to realize that inhomogeneities present in the propellant composition will have a more pronounced effect on the experimental stress-strain data, as was explained in [1].

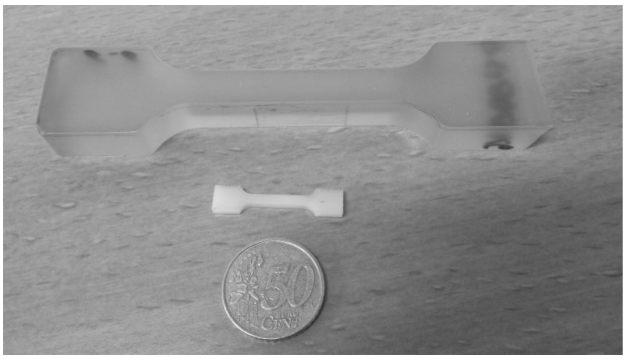

Figure 1. Comparison of the standard JANNAF C specimen (top), the one-quarter JANNAF specimen size used in this study (middle), and a 50 Euro cent coin (bottom). The specimens shown here are inert samples.

2.2 Equipment

2.2.1 Tensile/Compression Module

Similar to the previous study [1], a tensile/compression module from Kammrath and Weiss was also used to investigate the failure mechanism of the solid propellant in this study, see Figure 2. A one-quarter sized JANNAF test specimen is mounted between the two yokes, which can be moved symmetrically away from each other. Details on the device can be found in [1].

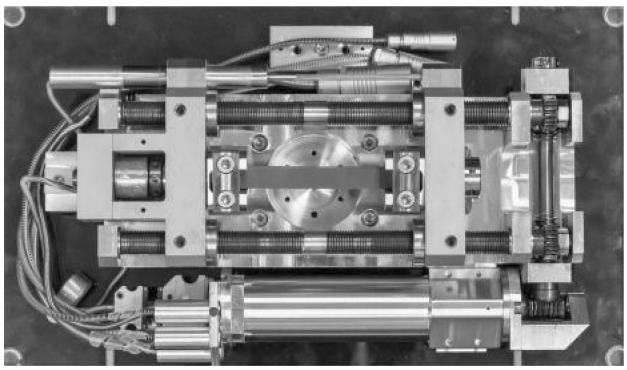

Figure 2. The tensile module which is sufficiently small to be mounted within a SEM for in-situ observation of the mechanical response of a specimen under tensile load.

2.2.2 Scanning Electron Microscopy (SEM)

In this study a FEI NovaNanoSEM 650 was utilized. The SEM combines a secondary electrons/back-scattered electrons (SE/BSE) in-lens detection and beam deceleration, and high sensitivity retractable SE/BSE and scanning transmitting electron microscopy (STEM) detectors. Both high (10^{-4} Pa) and low vacuum (10–200 Pa) modes, each mode with a different detector, were utilized in this study. The Everhart-Thornley detector (ETD) is operated in high vacuum, and the gaseous analytical detector (GAD) is used in low vacuum mode. The functioning of these two detectors has been described in detail in [9].

During experimentation magnifications were used that are comparable to the magnifications typically used in optical microscopy. In this way the entire width of the samples could be observed during the experiments. The different SEM detectors used, significantly enhanced the contrast between the different components in the propellant sample compared to optical microscopy.

2.2.3 Measurement of Glass Transition Temperature

The glass transition temperature, T_g, of a propellant marks the temperature at which the polymer matrix changes from a glassy ($T < T_g$) to a rubbery ($T > T_g$) state. For the measurement of the T_g a Dynamic Mechanical Analysis DMA/SDTA 861e from Mettler Toledo was used. After cooling down the sample to −80 °C, it was heated at a heating rate of 2 °C/min to 25 °C. The applied force was 5 N and the displace-

ment was 1 μm. Measurements were performed in duplicate at a frequency of 100 Hz.

2.3 Experimental Procedure

The tensile module was placed within the SEM chamber, and an HTPB/AP/Al propellant test specimen was placed into the sample holder of the module for each experimental test run. The tensile/compression module was controlled by the software on a computer outside of the SEM. All experiments were conducted at a constant strain rate of 150 μm/min, but the temperature was varied (−54, +25 and +40 °C). In order to conduct the experiments at different temperatures, the proper hardware must be set-up inside and outside of the SEM. For experiments conducted at a sample temperature of −54 °C, the heating element and stainless steel tubing for cooling fluid was placed within the SEM in addition to the tensile module. Liquid nitrogen was used as the coolant fluid and flowed through the stainless steel tubing from a pressure chamber outside of the SEM. The heating element was utilized to offset the liquid nitrogen cooling by helping to control the cooling rate and maintain the desired temperature. Due to the low thermal conductivity of the propellant composition material (0.4 $Wm^{-1}K^{-1}$), the propellant samples were exposed to a temperature of −54 °C for two hours in order to ensure the entire sample reached this low temperature prior to conducting the uniaxial tensile test. For experiments conducted at a sample temperature of +40 °C, the heating element was placed within the SEM in addition to the tensile module. The stainless steel tubing for cooling fluid was not needed during these elevated temperature experiments. The low thermal conductivity also had an effect on heating up the propellant sample to +40 °C, therefore the propellant samples were exposed to a temperature of +40 °C for one hour in order to ensure the sample reached desired temperature prior to conducting the uniaxial tensile test. For experiments conducted at a sample temperature of +25 °C, only the tensile module was needed to be placed within the SEM.

The strain rate of 150 μm/min was kept constant from the start of the experiment up to the point of rupture of the specimen. During each tensile test run, the load exerted (N), elongation of the specimen (μm), sample temperature (°C), and time (seconds) were recorded. Simultaneously the stress (mm/mm) and strain (MPa) were calculated using the cross-sectional area (7.2 mm^2) and length of the specimen (12.5 mm). While the sample was undergoing tensile stress, SEM images and videos were captured at set locations of the samples, while the sample was subjected to tensile stress. These images allowed for an in-situ view of the effects of tensile stress and temperature on the specimens and their components.

3 Results and Discussion

As explained in [1], a series of calibration runs were performed prior to conducting the experiments in this study.

HTPB/AP/Al propellant specimens were tested under tensile stress at three different temperatures at a constant strain rate of 150 μm/min within the SEM. Each test run was conducted according to the experimental procedure explained in Section 2.3. Stress as a function of strain of the HTPB/AP/Al propellant specimens at these three temperatures are shown in Figure 3. The stress and the strain data of phenomena occurring in the specimen have been summarized in Table 2.

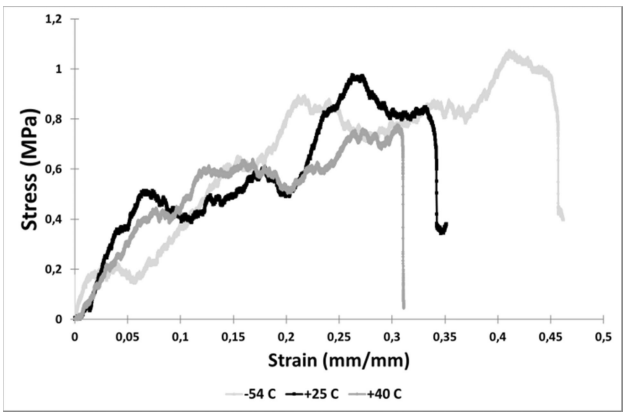

Figure 3. Stress-strain diagrams of HTPB/AP/Al propellant at a strain rate of 150 μm/min at −54, +25 and +40 °C.

Table 2. Mechanical properties taken from Figure 3 for each temperature.

T [°C]	E [MPa]	σ_{max} [MPa]	ε_{max} [mm/mm]	σ_{break} [MPa]	ε_{break} [mm/mm]
−54	13.2	1.069	0.412	0.915	0.451
+25	8.07	0.967	0.262	0.776	0.338
+40	5.75	0.769	0.306	0.725	0.310

While conducting the tensile experiments, in-situ SEM observance was used to understand the effect of tensile stress on the HTPB/AP/Al propellant specimens. The ETD and GAD detectors of the SEM were utilized to collect in-situ images and in-situ videos of the propellant specimens undergoing uniaxial tensile stress. However, the SEM GAD could only be used for experiments conducted at +25 °C due to the amount of space the heating element and stainless steel tubing take up within the SEM for the −54 °C and +40 °C experiments. Some of these images are shown in Figure 4. The trends in the mechanical properties E (Young's modulus, determined from the first linear part of the stress-strain curves in Figure 3), σ_{max} and σ_{break} as a function of temperature summarized in Table 2 agree with those gen-

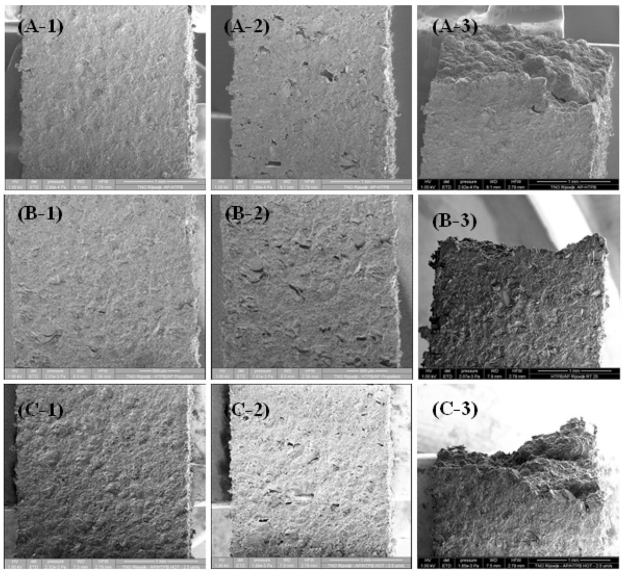

Figure 4. SEM images captured during in-situ uniaxial tensile tests conducted at a strain rate of 150 μm/min conducted at: (A) −54 °C; (B) +25 °C; and (C) +40 °C. The number in the upper left corner of each picture corresponds with the following positions in Figure 3 and Table 2: (1) Yield Stress/Strain; (2) Maximum Stress/Strain; (3) Rupture/Break. The images were recorded with ETD in high vacuum.

erally found on macroscale, since these values are generally found to increase with decreasing temperature [2]. The increase in *E* for lower temperatures implies that the polymer matrix behaves more stiff than at higher temperatures. This is related to the restriction in the mobility of the polymer molecules at low temperature. A Young's modulus in the range of 5–10 MPa, as was found at +25 and +40 °C, is a typical value for this type of propellant. However, at −54 °C one normally would expect values around 100 MPa. The much lower value of 13.2 MPa might indicate that the temperature of the sample was higher, due to heat influx from the surrounding. As a result of the strong temperature dependence of the elastic modulus at low temperatures, a relatively small increase in sample temperature might already cause a significant decrease in the value of *E*. Furthermore, the sample has a very low thermal conductivity, so heat transfer takes quite a long period of time especially in vacuum. The values for ε_{break} as a function of temperature show a reversed trend compared to testing at macroscale, since this value is normally found to decrease when temperature is lowered. Also values for ε_{max} do not show a clear trend. This might be an effect of the smaller dimensions of the one-quarter sized dogbones relative to the mean size of the AP particles (ca. 200 μm) in the propellant, which enhances the influence of inhomogeneities in the sample on the mechanical properties compared to the full-size dogbones used in macroscale testing.

The SEM ETD images were able to show an excellent representation of the full width of the specimens. Poisson's effect on the specimens was observed in the SEM ETD images, as seen in Figure 4. As the specimens elongated, their width decreased, and this is evident when comparing images A-1 to A-2, B-1 to B-2, and C-1 to C-2 in Figure 4.

During the low temperature tensile experiments (−54 °C), the HTPB binder matrix behaved much more rigid than during the experiments conducted at +25 and +40 °C. The cracks and voids initiated from the tensile stress were concentrated around the larger AP particles, and the number of cracks and voids formed in the bulk of the HTPB binder matrix was lessened due to its rigidity. The process of the rupture was also very different in the low temperature experiments than at +25 °C and +40 °C. While the HTPB binder matrix slowly pulled apart in a similar fashion to chewing gum during the elevated temperature tensile experiments, the HTPB binder matrix snapped at rupture during the −54 °C tensile experiments. The rubbery rather than brittle or glassy behavior of the propellant prior to its sudden rupture, showed that it was still above the glass transition temperature during the −54 °C conditions. The glass transition temperature T_g of this propellant, as measured with DMA, was found to be −60 °C, confirming that the low temperature measurements were conducted slightly above the glass transition temperature of the propellant.

4 Conclusions

In-situ uniaxial tensile experiments of HTPB/AP/Al propellant specimens were successfully conducted within a SEM at −54, +25 and +40 °C. Each experiment included real-time observation at the micron-level of the specimen and digital recording of the stress and strain values. The stress-strain diagrams were affected by the sample temperature. The trends in the Young's modulus, σ_{max} and σ_{break} as a function of temperature agree with those generally found on macroscale. However, the values for ε_{break} as a function of temperature show a reversed trend compared to testing at macroscale. Also values for ε_{max} do not show a clear trend. This might be related to the smaller dimensions of the one-quarter sized dogbones relative to the mean size of the AP particles (ca. 200 μm) in the propellant, which enhances the influence of inhomogeneities in the sample on the mechanical properties compared to the full-size dogbones used in macroscale testing.

Stress relaxation of the specimens was present in the stress-strain diagrams due to nucleation of cracks and voids in the specimen during experimentation. The in-situ SEM observance, images and videos confirmed the nucleation and growth of cracks and voids in all of the specimens.

By recording in-situ SEM images and videos, the interface of the HTPB binder matrix and the AP particle were found to be the main source of failure in the HTPB/AP/Al propellant specimens while under tensile stress. However, the experiments conducted at −54 °C showed a different

failure behavior of the propellant sample due to its rigidity at this low temperature, while experiments conducted at $+25$ and $+40\,^{\circ}C$ displayed a similar failure mechanism. The cracks and voids initiated from the tensile stress were concentrated around the larger AP particles, and compared to the elevated temperatures, less cracks and voids were formed in the bulk of the HTPB binder matrix to its rigidity. While the HTPB binder matrix slowly pulled apart in a similar fashion to chewing gum during the elevated temperature tensile experiments, the HTPB binder matrix snapped at rupture during the $-54\,^{\circ}C$ tensile experiments. The behavior of the propellant showed that it was still above the glass transition temperature during the $-54\,^{\circ}C$ conditions. This was confirmed by DMA measurements giving a glass transition temperature of $-60\,^{\circ}C$. For future testing using this tensile tester, special attention should be given to improved temperature control of the specimen, especially at low temperatures.

Acknowledgements

The authors would like to thank Peter Kuivenhoven (TNO) for providing the experimental samples used in this study. The authors would also like to thank Frans-Peter Weterings (TNO) for providing the propellant, indicating propellant properties, and sharing his experience with macrotensile testing.

References

[1] M. C. J. van Ramshorst, G. L. Di Benedetto, W. Duvalois, P. A. Hooijmeijer, A. E. D. M. van der Heijden, Investigation of the Failure Mechanism of HTPB/AP/Al Propellant by In-Situ Uniaxial Tensile Experimentation in SEM, *Propellants Explos. Pyrotech.* **2016**, *41*, 700–708.

[2] H. Shekhar, Effect of temperature on mechanical properties of solid rocket propellants, *Defence Science Journal* **2011**, *61*, 529–533.

Received: July 11, 2017
Revised: September 21, 2017
Published online: October 12, 2017

